Final Technical Report

Molecularly Engineered Energy Materials

DOE Office of Science, Basic Energy Sciences Energy Frontier Research Center (EFRC)

DOE Award Number: DE-SC0001342

EFRC Director: Vidvuds Ozolins
Email: vidvuds@ucla.edu
Phone: (310) 267-5538
Fax: (310) 206-7353

Date of report: September 28, 2016

Period covered by the report: August 1, 2009 – July 31, 2015

Lead Institution:

University of California, Los Angeles
420 Westwood Plaza
Los Angeles, California 90095

Participating Institutions:

University of California, Los Angeles (UCLA)
University of California at Berkeley (UC Berkeley)
University of Kansas (KU)
Eastern Washington University (EWU)
National Renewable Energy Laboratory (NREL)
Lawrence Berkeley National Laboratory (LBNL)
University of Washington, Seattle (UW Seattle)

Senior Principal Investigators:
Mark Asta (UC Berkeley, mdasta@berkeley.edu)
Bruce Dunn (UCLA, bdunn@ucla.edu)
Samson Jenekhe (UW Seattle, jenekhe@u.washington.edu)
Nikos Kopidakis (NREL, nikos_kopidakis@nrel.gov)
Yao Houndonougbo (EWU, yhoundonoug@ewu.edu)
Brian Laird (KU, blaird@ku.edu)
Yunfeng Lu (UCLA, luucla@ucla.edu)
Daniel Neuhauser (UCLA, dxn@chem.ucla.edu)
Laurent Pilon (UCLA, pilon@seas.ucla.edu)
Yves Rubin (UCLA, rubin@chem.ucla.edu)
Benjamin J. Schwartz (UCLA, schwartz@chem.ucla.edu)
Sarah H. Tolbert (UCLA, tolbert@chem.ucla.edu)

1 TECHNICAL ACCOMPLISHMENTS

Molecularly Engineered Energy Materials (MEEM) was established as an interdisciplinary cutting-edge UCLA-based research center uniquely equipped to attack the challenge of rationally designing, synthesizing and testing revolutionary new energy materials. Our mission was to achieve transformational improvements in the performance of materials via controlling the nano- and mesoscale structure using selectively designed, earth-abundant, inexpensive molecular building blocks. MEEM has focused on materials that are inherently abundant, can be easily assembled from intelligently designed building blocks (molecules, nanoparticles), and have the potential to deliver transformative economic benefits in comparison with the current crystalline- and polycrystalline-based energy technologies.

MEEM addressed basic science issues related to the fundamental mechanisms of carrier generation, energy conversion, as well as transport and storage of charge and mass in tunable, architectonically complex materials. Fundamental understanding of these processes will enable rational design, efficient synthesis and effective deployment of novel three-dimensional material architectures for energy applications. Three interrelated research directions were initially identified where these novel architectures hold great promise for high-reward research: solar energy generation, electrochemical energy storage, and materials for CO_2 capture. Of these, the first two remained throughout the project performance period, while carbon capture was been phased out in consultation and with approval from BES program manager.

1.1 Capacitive energy storage

Capacitive energy storage technology is based on electrochemical capacitors (ECs), also called supercapacitors, which store energy by either ion adsorption (electrochemical double layer capacitors) or fast surface redox reactions (pseudocapacitors). **Figure 1** shows the power and energy relationship between the two leading electrical energy storage technologies, batteries and electrochemical capacitors. An interesting feature in this traditional graphic is that supercapacitors bridge the gap between high energy density and high power density (i.e., between batteries and traditional capacitors). The success of lithium-ion batteries over the past two decades in consumer electronics and, more recently, the first generation of plug-in hybrids, has led to a number of advances in energy storage technology. Nonetheless, capacitive storage offers a number of desirable properties: fast charging (within seconds), reliability, long-term cycling (>500,000 cycles), and the ability to deliver more than 10× the power of batteries. As a result, capacitive storage has become an important energy storage technology for applications where a large amount of energy needs to be either stored or delivered quickly. These include kinetic energy harvesting in seaports[1] or with regenerative braking;[2] pulse power in communication devices;[3] and power quality applications in the electrical grid.[4] In addition, shorter charging times would be very convenient for portable devices and especially for electric vehicles. The limiting feature that prevents more widespread usage of ECs has been the relatively low energy density of the materials used in capacitive storage applications.

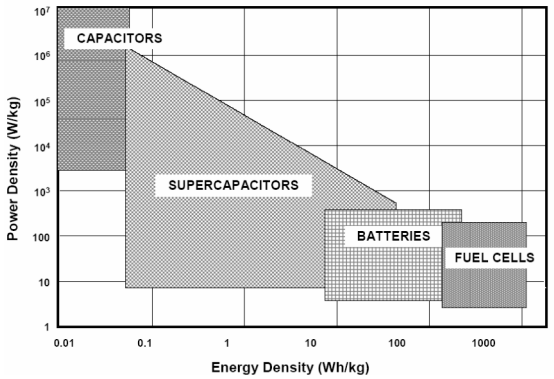

Figure 1. Supercapacitors are intermediate between batteries and capacitors in both energy and power density.

Electrical double layer capacitors: Electrochemical double layer capacitors (EDLCs) serve as the basis for the current technology in capacitive energy storage.[5] Charge storage occurs through the adsorption of electrolyte ions onto the surfaces of electrified materials. Carbons are ideal EDLC electrode materials due to the combination of high conductivity, large surface area, and low density. This type of charge storage is electrostatic and no redox reactions are involved. Thus, the charge can be quickly discharged or charged, but the amount of charge stored at the interface is limited. The field of EDLCs has been the subject of numerous reviews over the past few years.[6-8] Currently, the best carbon materials achieve double-layer capacitances of approximately 150 F g^{-1} for optimum carbon pore sizes in ionic liquid electrolytes.[9] The prospect of using graphene for EDLCs has generated considerable interest in the field as the high surface area of graphene has led to specific capacitances in the range of 100-250 F g^{-1}.[10,11] In recent years, there has been considerable effort aimed at increasing specific energy of EDLCs without compromising specific power, and there are reports of energy density values reaching 10 Wh/kg in energy storage devices that provide 1 Farad or greater.

Pseudocapacitor Materials: The MEEM program is concerned with transition metal oxide materials that exhibit pseudocapacitance, which occurs when reversible redox reactions take place at or near the surface of a material in contact with an electrolyte. The interest in using pseudocapacitive materials for electrochemical capacitors is that the energy density associated with faradaic reactions is much higher, by at least an order of magnitude, than traditional double layer capacitance (above 100 μF/cm^2 for pseudocapacitance *vs.* 10 to 20 μF/cm^2 for EDLCs). The origin of pseudocapacitance was described thoroughly by Conway[12] who identified three faradaic mechanisms that can result in capacitive electrochemical features:[7] underpotential deposition, redox pseudocapacitance (as in $RuO_2 \cdot nH_2O$) and intercalation pseudocapacitance. The latter two effects are of interest for capacitive energy storage. Redox pseudocapacitance occurs when ions are electrochemically adsorbed onto and/or near the surface of a material with a concomitant faradaic charge transfer. Intercalation pseudocapacitance occurs when ions intercalate into the channels or layers of a redox-active material accompanied by a faradaic charge-transfer with no crystallographic phase change. These three mechanisms arise from different physical processes and with different types of materials; the similarity in the electrochemical signatures occurs due to the relationship between the potential and the extent of charge that develops as a result of adsorption/desorption processes at the electrode/electrolyte interface or within the inner surface of a material:[13]

$$E \approx E^0 - \frac{RT}{nF} \ln\left(\frac{X}{1-X}\right). \quad (1)$$

Here, E is the potential (V), R is the ideal gas constant (8.314 J mol^{-1} K^{-1}), T is the temperature (K), n is the number of electrons, F is the Faraday constant (96,485 C mol^{-1}), and X is the extent of fractional coverage of the surface or inner structure. A specific capacitance (C in F g^{-1}) may be defined in regions where the plot of E *vs.* X is linear:

$$C = (nF/m)X/E, \quad (2)$$

where m is the molecular weight of the active material. Since $E(X)$ is not entirely linear as in a capacitor, the capacitance is not always constant, and so it is termed pseudocapacitance.

Despite the advantages of having faradaic reactions, prior work with pseudocapacitive materials has brought to light an important question about reaching the very high theoretical values of the

pseudocapacitive systems. The specific capacitance, based on either 1-electron or 2-electron redox reactions, is very high for systems such as V_2O_5, NiO and MnO_2, well above 1000 F/g.[14-16] These high values have been demonstrated using nanoscale forms of these materials and specially designed electrode structures which ensure that most of the electrochemically active transition metal oxide is exposed to electrolyte and participates in the reaction. However, standard composite electrode approaches are not as effective as specific capacitance values are typically in the range of 150 to 250 F/g.[17] Accordingly, one of the central scientific gaps we are addressing in the MEEM program is the development of electrode architectures which retain high specific capacitances and offer a practical electrode structure for capacitor devices.

The MEEM program on capacitive energy storage is a comprehensive one which combines experimental and computational components to achieve a fundamental understanding of charge storage processes in redox-based materials, specifically transition metal oxide systems. As indicated above, these materials are a particularly appealing target because, with few exceptions, theoretical values of their specific capacitance (F g^{-1}) are several times greater than experimentally achieved results. It is, therefore, a topic where improved fundamental understanding of pseudocapacitive materials can have a dramatic impact on the field.

A central theme for the experimental studies is to create pseudocapacitor materials with appropriate nanoscale architecture. Accordingly, we have emphasized the study of template-directed mesoporous transition metal oxides in which the interconnected pore network provides electrolyte access to the high surface area, electrochemically active walls. Provided the films are sufficiently thin (less than 100 nm) there is adequate electronic conductivity for the redox reactions. Moreover, these architectures provide an ideal platform for determining the fundamental pseudocapacitor properties of different inorganic systems because the resulting films contain neither carbon nor binder. Thus, we directly determine the fundamental electrochemical properties of the pseudocapacitive material. With this method, we were able to determine the pseudocapacitive properties of various materials[18] and readily identified Nb_2O_5 to have exceptionally rapid charge storage properties.[19]

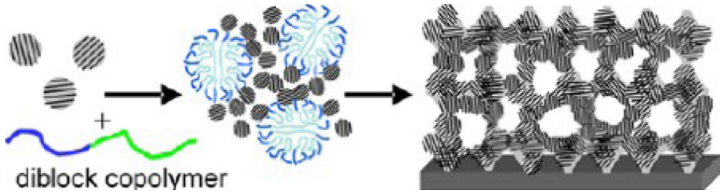

Figure 2. Process for synthesizing mesoporous films where nanocrystal building blocks co-assemble with polymer templates. Upon heating the polymer decomposes leaving behind the mesoporous film. From Ref. 20.

In more recent work, we developed a new route for synthesizing mesoporous films in which preformed nanocrystal building blocks are used in combination with polymer templating.[20] The general synthetic route is shown in **Figure 2**. A significant advantage of this route is that we are now able to evaluate a much wider range of redox active materials than was possible with the sol-gel derived systems used to date. In addition, we are able to prepare films comprised of smaller crystalline domains with higher surface area, characteristics that should be beneficial for obtaining pseudocapacitive responses. The first pseudocapacitive films prepared by this route show considerable promise.

As indicated above, the results with Nb_2O_5 mesoporous films indicated that not only was Li^+ insertion extremely rapid, but that this material possesses much better charge storage kinetics than other transition metal oxides.[21] Moreover, the orthorhombic phase in particular was found to

exhibit high specific capacitance at high rate with values of nearly 450 F/g achieved in less than 1 minute, far superior to the corresponding mesoporous amorphous films (**Figure 3**). Such rapid charge storage is enabled by the structure of *T*-Nb_2O_5, which consists of sheets of corner- or edge-sharing Nb^{+5} polyhedra along the (001) plane that are coordinated by six or seven O^{2-}. Density-functional theory (DFT) studies indicate that the (001) plane exhibits low energy barriers for lithium ion transport and gives rise to the pseudocapacitive behavior observed in this material.

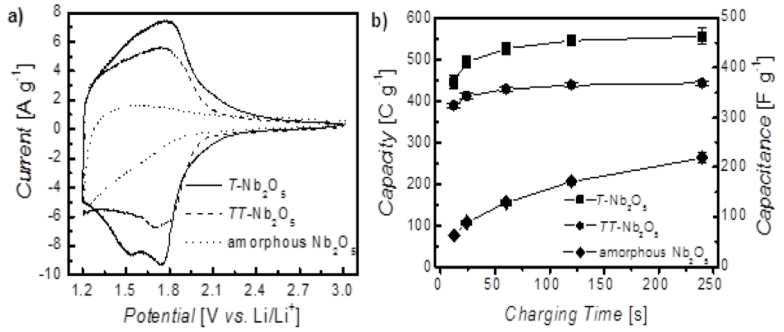

Figure 3. Voltammetric sweeps for Nb_2O_5 in lithium ion electrolyte: a) CVs at 10 mV s^{-1} for different Nb_2O_5 phases and b) charge storage as a function of charging time for the same materials. The *T*-phase demonstrates the highest level of charge storage capacity for all sweep rates investigated. From Ref. 21.

In more recent work, we were able to attribute the high level of energy storage at high rates in Nb_2O_5 to an intercalation pseudocapacitance mechanism.[22] Its characteristic electrochemical features include currents that vary inversely with time, charge-storage capacity that is mostly independent of rate and redox peaks that exhibit small voltage offsets, and therefore good reversibility, at high rates. Kinetic studies indicate that for charging times of 1 minute or longer, there are no indications of ionic diffusion limitations and the current response is capacitor-like.[22] Another key design rule for intercalation pseudocapacitance is that the structure does not undergo a phase transformation upon intercalation.

We have begun to investigate the properties of Nb_2O_5 in traditional composite electrodes in which carbon and binder are mixed with the active material. Not only does the composite material continue to exhibit intercalation pseudocapacitance features as listed above, but we incorporated these composite electrodes in asymmetric devices whose energy and power densities surpass those of commercial EDLC devices.[23] In the proposed program, we will be using Nb_2O_5 as a model material for transient absorption experiments, core-shell experiments and in designed electrode architectures. Nb_2O_5 will serve as a key benchmark for determining intercalation pseudocapacitance in other transition metal systems that we plan to investigate.

We also 're-discovered' another fast-ion conducting system, the hydrated form of hexagonal WO_3. In this case the mobile ions are protons. The electrochemical characteristics for the hydrated h-WO_3 are similar to those of Nb_2O_5 in terms of there being only small changes in capacitance with sweep rate with no evidence of diffusion limitations until very high discharge rates. In this system, protons move through one-dimensional (1D) channels lined with water molecules, and no phase transformation occurs as the proton/metal atom ratio approaches one. This charge storage process is very different from other proton-conducting pseudocapacitive materials, such as hydrous RuO_2, in which redox reactions occur at the surface. The bulk nature of charge storage in h-WO_3 makes this material very appealing for applications in charge storage, as well as for making electron- and proton-conducting membranes. We will not further pursue h-WO_3 here, since this topic has been successfully 'spun-off' into an ARPA-E project

"Long-Life, Acid-Based Battery" in the Robust Affordable Next Generation EV-Storage (RANGE) program.

The MEEM program has had a very active effort, led by the **Pilon** group, directed at developing physical models and accurate numerical tools to describe how the electrode/electrolyte interface and electrochemical properties of electrochemical capacitors are influenced by electrode morphology. They worked with both equilibrium models, such as the Modified Poisson-Boltzmann (MPB) model[24,25] as well as dynamic models, such as the Modified Poisson-Nernst-Planck (MPNP) model.[26] This group has advanced the computation area for supercapacitors significantly by developing new boundary conditions that rigorously account for interfacial phenomena at the electrode/electrolyte interface and enable simulations of actual 3D mesoporous electrodes. They developed numerical tools that were able to reproduce typical electrochemistry experiments including cyclic voltammetry (CV),[27] impedance spectroscopy,[28,29] and galvanostatic cycling[30] measurements. In addition, these models gave new insights to the measurements so that the **Pilon** group was able to provide physical interpretations for experimental results. Scaling analysis was systematically performed and the resulting similarity parameters reduced the number of variables and were used to identify diffusion-limited operation, and design rules for both electrodes and electrolytes. These initial studies were carried out with carbon-based materials (EDLCs) so that it would be possible to validate the models with experimental results from the literature. But now that redox-active systems are being addressed, collaboration between computational and experimental groups is well established and the models being developed are for the materials being investigated within MEEM. These methodologies form the basis for the multiscale modeling which plays a key role in the electrode architecture section of our proposal.

1.2 Organic photovoltaics

Sunlight is the most abundant, renewable, and non-polluting energy resource available to humans and yet it remains one of the most poorly utilized. Solar cells incorporating crystalline materials currently provide the highest efficiencies for solar energy conversion to electricity, but their widespread adoption remains limited due to high production costs. Hence, less expensive photovoltaics based on polycrystalline thin films are becoming increasingly popular.

In the first period of MEEM, we investigated several self-assembly based strategies for controlling the morphology of solution processes organic photovoltaic (OPV) cells, including the use of self-stacking shuttlecock fullerenes, amphiphilic semiconducting polymers, and sequentially processed (SqP) solar cells. Since then, OPV has emerged as an established technology, which routinely achieves 10% power conversion efficiency in the lab.

One of our major efforts over the last several years has been to circumvent the kinetic sensitivities involved in forming an optimal bulk heterojunction (BHJ) morphology in organic solar cells. To this end, we have used sequential processing, self-assembling fullerenes, and self-assembling polymers to enhance OPV performance.

We have developed a new method, known as sequential processing (SqP), as a means to control OPV morphology.[31-35] SqP is based on sequential deposition of the donor and acceptor molecules via casting from orthogonal solvents. A typical SqP device might have the polymer layer (e.g., P3HT) cast from a solvent such as *o*-dichlorobenzene, followed by casting the fullerene layer (e.g., PCBM) from dichloromethane. In our initial work, we had concluded that SqP led to a bilayer structure,[31] but later work from both our group using TRMC[32] and other groups using

neutron reflection[36-39] and other techniques[40-47] has shown that there is interpenetration of the fullerene from the overlayer into the polymer underlayer. Subsequently, dozens of groups have worked to explore the differences between devices made as traditional BHJs and via SqP,[42,45-59] particularly since SqP provides the ability to alter the donor layer prior to fullerene deposition. SqP also provides for greater reproducibility in the performance of polymer-based PVs, particularly as the device area is increased. This is because SqP avoids problems with the kinetics of phase separation of the two components and/or issues with differential solubility of the components in the casting solvent.[34]

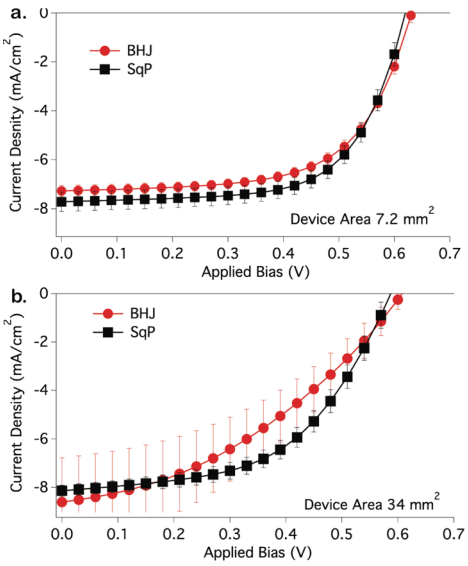

Figure 4. Thickness- and composition-matched BHJ and SqP P3HT/PCBM solar cells with small (a) and large (b) areas. Error bars are ±1σ (20 devices).

For example, **Figure 4**a compares the photovoltaic performance of two sets of small-area (~7 mm^2) devices with the same active layer thickness and the same molar composition of P3HT and PCBM; one set prepared as a BHJ by blending the components in solution first, and the other prepared by SqP. The two sets of devices behave similarly. When the same solutions are used to make films for larger-area (~34 mm^2) devices, however, **Figure 4**b shows that not only do the SqP devices perform better than BHJ devices, but they also perform more consistently: the error bars mark ±1 standard deviation in a sampling of over 20 devices of each type. Thus, SqP provides a significant step toward removing the irreproducibility that is inherent in the kinetic control of blend morphology when fabricating devices as BHJs.

One key question concerning SqP devices is: how does the fullerene penetrate into the polymer underlayer? For reasonably crystalline polymers like P3HT, devices built as BHJs have much less crystalline polymer than devices made by SqP. This is because the presence of the fullerene inhibits crystallization, as we have shown with XRD,[60,61] while in SqP, the polymer can crystallize without the hindering presence of fullerene.[62] Both we[33,35] and others[32,44-47,63,64] have argued that the fullerene in SqP intersperses only into the amorphous regions of the film, leaving the crystalline polymer regions intact. We have shown in recent work that even though polymer crystallinity enhances hole mobility, too much crystallization limits the amount of fullerene that incorporates into the film, reducing device performance.[33] **Figure 5**b shows the results of fabricating SqP films using conjugated polymers that were synthesized to have the same backbone but different degrees of crystallinity (via different degrees of regioregularity); clearly there exists an optimal crystallinity range in which the amorphous polymer fraction is sufficient to allow for efficient fullerene incorporation without driving phase separation into large aggregates or allowing for over-mixing of the polymer and the fullerene.[65] Thus, as shown in **Figure 5**a, devices made with P3HT with moderate crystallinity showed the best performance.

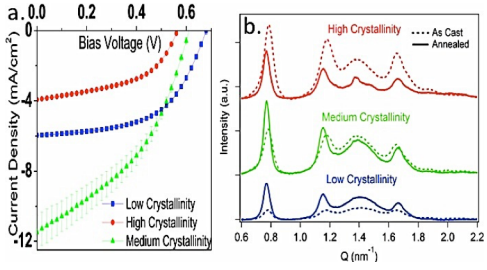

Figure 5. (a) *J-V* curves for annealed SqP devices with varying degrees of polymer crystallinity. (b) XRD of device active layers from part (a).

Another one of our major efforts over the last several years has been to circumvent the kinetic sensitivities involved in forming an optimal BHJ morphology using molecular self-assembly. To this end, we synthesized fullerene derivatives with molecular shapes resembling badminton shuttlecocks (SCs)[66] using the methodology of Nakamura.[67-69] Depending on the substituents, some SCs stack ball-in-cup, forming a 1-D columnar motif when crystallized in the solid state.[70] By varying the alkyl group size on the SC feathers, we were able to control the propensity of SCs to stack while keeping their electronic structure identical.[66,70] When used in OPV devices, we found that stacking SCs gave much higher currents compared to their non-stacking counterparts.[66,71] We then used time-resolved microwave conductivity (TRMC) to show that the local mobility (i.e. probability for e^- transfer between 2-3 adjacent fullerenes) was similar on stacking and non-stacking SCs. In addition, using theoretical techniques, we also found that the probability for local electron transfer was identical for the stacking and non-stacking SC derivatives.[72] This proves that stacking can improve global mobility.

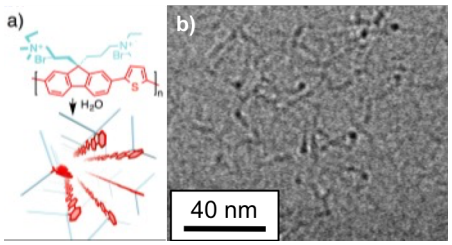

Figure 6. a) Chemical structure of PFT and its micelle formation in H_2O. b) Cryo-EM of PFT micelles.

In addition to enhancing OPV performance via newly designed self-assembling fullerenes, we have developed self-assembling conjugated polymers to control morphology and enhance hole transport.[73] To this end, we synthesized the amphiphilic semiconducting poly(fluorene-alt-thiophene) (PFT), shown in **Figure 6**a. We verified via solution small-angle x-ray scattering (SAXS), AFM, and cryo-TEM (**Figure 6**b) that PFT indeed assembles into long cylindrical micelles.[73] This geometry straightens the polymer chains along the long axis of the cylinder, resulting in increased conductivity along the backbone.[74] Indeed, we recently have shown that amphiphilic PFT diodes have significantly enhanced currents compared to diodes based on an uncharged and thus unassembled version of this same polymer.[73]

1.3 Carbon capture

Understand the effect of imidazolate functionalities on CO_2 uptake and selectivity in a class of ZIFs built from tetrahedrally coordinated Zn ions; Perform Monte-Carlo simulations of equilibrium uptake values as functions of temperature and pressure: We have completed our combined experimental/computational analysis of CO_2 uptake for an isoreticular series of 5 ZIF's with a RHO topology, but with a diverse range of functionalities, that was synthesized as part of this effort by the Yaghi group at UCLA (See Fig. 7). These five ZIFs (ZIF-25, -71, -93, -96, and -97) were synthesized by the reaction of $Zn(acetate)_2$ and the respective imidazole derivative in DMF. They vary only in the functionality that point into the pores of the framework, with a diverse range of functionalities including CH_3, -CHO, -CN, and $-NH_2$. This study was designed to help understand the role of functionality on ZIF carbon capture. In our simulations, we have also determined a number of other relevant quantities such as surface area and adsorption enthalpy. Agreement with experiment for these quantities is good.

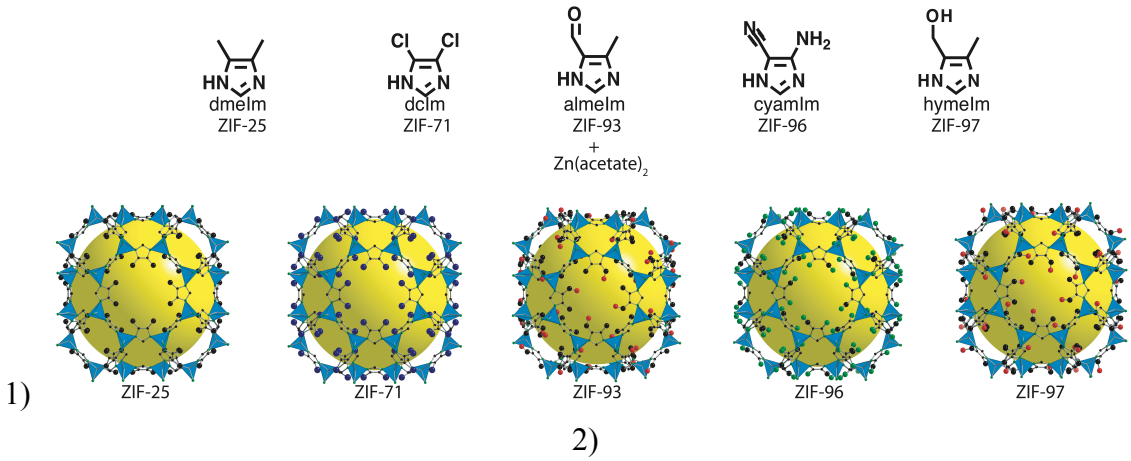

1)

2)

3) **Figure 7:** Synthesis of RHO ZIF materials

Perform MD simulations in the study of the diffusion coefficients of gas species in ZIF structures with different functionalization; develop a model of the kinetics of uptake of gas mixtures: Over the past year potential parameters and structure models were implemented into the LAMMPS MD code to calculate CO_2 diffusivities in the isoreticular set of rho-structured ZIFs described above. Test simulations were conducted to probe equilibration times, system size effects, and the choice of thermostat parameters on calculated diffusivities. Initial results have led to the identification of a number of distinct binding sites within the RHO-topology ZIFs, with significantly varying energy barriers for diffusion depending on the functionality.

Develop modeling techniques to systematically study the dependence on CO_2 uptake on the details of the framework/CO_2 interaction – especially with regard to the functionalization of the imidazole: Using the formalism of van der Waals density functional theory (vdW-DFT) we have undertaken an effort to use quantum-mechanical methods to optimize classical potential parameters for the ZIF MD and MC simulations. This effort has focused to date on ZIF-93 and 96 structures. For ZIF-93 available classical potentials yield adsorption isotherms in good agreement with measurements, while for ZIF-96 the calculated adsorptions are significantly lower than the experimental data. More importantly, from the standpoint of using calculations to guide the design of ZIFs for carbon capture applications, the available classical potentials do not predict the correct trend: ZIF-93 is predicted to have higher adsorption than -96, whereas the opposite is found experimentally; therefore, we are devoting significant effort to optimizing the force fields guided by electronic structure calculations.

Experimentally evaluate the ability of these ZIFs to uptake other gases, including CH_4 and CO: We have examined (both experimentally and computationally) the adsorption of CH_4 in the same isoreticular set of five ZIFs for which we have examined the CO_2 adsorption in detail. The original set of force field parameters, based on the UFF potential with charges, that we used for CO_2 was found to be inadequate for predicting the adsorption of methane. Therefore, we put considerable effort into designing new force field parameters that give reasonable results in comparison with experiment for both CO_2 and CH_4. This allows us to make predictions on CO_2/CH_4 selectivity. This work is the subject of a manuscript in preparation. Water being an important component of flue gases, we have also examined the effect of water loading on CO_2 and CH_4 adsorption and selectivity in a number of candidate ZIFs.

Investigate other known ZIF topologies to access their ability for gas uptake: To do this we had to keep other variables including imidazolate and metal ion constant. The first example we choose to study is that of ZIF-93 and ZIF-94. Both of these ZIFs are comprised of the same imidazolate, but possess different topologies RHO and SOD. The pore sizes of the SOD cage are smaller than the RHO cage, giving us the opportunity to see how this affects gas adsorption.

Explained effect of functionalization on adsorption of CO_2, CH_4 and H_2O in ZIFs: The principal finding was that the composition and symmetry of the functionalization has significant effects on CO_2 and CH_4 adsorption in these ZIFs. In the case of CH_4 adsorption uptake was proportional to surface area, but in CO_2 the uptake was significantly enhanced in ZIFs with asymmetrically functionalized imidazoles (ZIF-93,-96, and -97). Also, the computational studies show that the adsorption of both CO_2 and CH_4 occurs primarily in the smaller hexagonal bridging channels of these ZIFs and not in the larger octahedral pore. The experimental and simulation results on this series for the adsorption of CO_2 were subsequently published as a JACS communication. Our results for the adsorption of CH_4 are the subject of a combined experimental/computational paper in preparation. Results from our water loading studies show that the presence of water decreases the adsorption of CO_2 and CH_4 and the selectivity for CO_2 by a few percent up to 1 bar partial pressure, with the largest effects coming at higher CO_2/CH_4 pressures (near 1 bar) and higher relative humidities.

Explained effect of topology on CO_2 adsorption: At pressures below 100 kPa enhanced adsorption of CH_4 and CO_2 was measured experimentally in ZIF-93 versus -94, which have identical imidazolate functionality, but different topologies (RHO versus SOD, respectively). These measurements are supported by computational results that show enhanced adsorption in the smaller SOD pores; however, the computational studies also show that the adsorption of CH_4 is enhanced to a greater degree than CO_2, so that smaller pores lead to a decreased CO_2/CH_4 selectivity

Development of vdw-DFT-based force fields: Binding energies of CO_2 at different sites within ZIF-93 and –96 were calculated using the vdW-DFT functional developed by Langreth and co-workers, and the results were used to refit the ε parameters in the Lennard-Jones potentials. The resulting potentials gave rise to calculated adsorptions for ZIF-96 in much better agreement with experimental data, and reproduced the measured trend that this structure has higher uptake than ZIF-93. Initial results of this work have been presented by one of the students supported by the EFRC at the March APS meeting and the Spring MRS meeting.

Diffusion of CO_2 in ZIFs: An important finding was the identification of multiple sites within the structures where CO_2 molecules are strongly bound, and have high activation energies for escape. At high uptakes these sites are largely filled, and the diffusion flux is dominated by molecules that interact relatively weakly with the framework. At low concentrations, diffusion constants are expected to be controlled by the slow hopping rates of molecules out of the strong binding sites. Simulations have been completed for CO_2 tracer and transport diffusion constants in ZIF-25, -71, -93 and -97, at concentrations corresponding to equilibrium adsorptions at a pressure of 101 kPa, at 298 K.

REFERENCES

1. J. R. Miller and P. Simon, "Electrochemical Capacitors for Energy Management," *Science* **321**, 651 (2008)
2. R. Kötz, "Principles and applications of electrochemical capacitors," *Electrochim. Acta* **45**, 2483 (2000).

3. R. Huggins, Supercapacitors and electrochemical pulse sources, *Solid State Ionics* **134**, 179 (2000).
4. B. Dunn, H. Kamath, and J.-M. Tarascon, "Electrical energy storage for the grid: a battery of choices," *Science* **334**, 928 (2011).
5. B. E. Conway and W. G. Pell, "Double-layer and pseudocapacitance types of electrochemical capacitors and their applications to the development of hybrid devices," *J. Solid State Electrochem* **7**, 637 (2003).
6. R. Signorelli, D. C. Ku, J. G. Kassakian, and J. E. Schindall, "Electrochemical Double-Layer Capacitors Using Carbon Nanotube Electrode Structures," *Proc. IEEE* **97**, 1837 (2009).
7. P. Simon and A. Burke, "Nanostructured Carbons: Double-Layer Capacitance and More," *Electrochem. Soc. Interface* **2008**, 38–43.
8. L. L. Zhang and X. S. Zhao, "Carbon-based materials as supercapacitor electrodes," *Chem. Soc. Rev.* **38**, 2520 (2009).
9. P. Simon and Y. Gogotsi, **"**Materials for electrochemical capacitors," *Nat. Mater.* **7**, 845 (2008).
10. Y. Huang, J. Liang, and Y. Chen, Supercapacitors, an overview of the applications of graphene-based materials in supercapacitors," Small **8**, 1805 (2012).
11. W.-Y. Tsai, R. Lin, S. Murali, L. L. Zhang, J. K. McDonough, R. S. Ruoff, P.-L. Taberna, Y. Gogotsi, and P. Simon, "Outstanding performance of activated graphene based supercapacitors in ionic liquid electrolyte from-50 to 80° C," *Nano Energy* **2**, 403 (2013).
12. B.E. Conway, V. Birss and J. Wojtowicz, "The role and utilization of pseudocapacitance for energy storage by supercapacitors," *J. Power Sources* **99**, 1 (1997).
13. B. E. Conway, "Two-dimensional and quasi-two-dimensional isotherms for Li intercalation and upd processes at surfaces," *Electrochim. Acta* **38**, 1249 (1993).
14. I.-H. Kim, J.-H. Kim, B.-W. Cho, and B-W. Kim, "Pseudocapacitive properties of electrochemically prepared vanadium oxide on carbon nanotube film substrate," *J. Electrochem. Soc.* **153**, A1451 (2006).
15. K.-W. Nam, E.-S. Lee, J.-H. Kim, Y.-H. Lee, and K.-B. Kim, "Synthesis and electrochemical investigations of Ni1-xO thin films and Ni1-xO on three-dimensional carbon substrates for electrochemical capacitors," *J. Electrochem. Soc.* **152**, A2123 (2005).
16. M. Toupin, T. Brousse, and D. Belanger, "Charge storage mechanism of MnO_2 electrode used in aqueous electrochemical capacitor," *Chem. Mater.* **16**, 3184 (2004).
17. T. Cottineau, M. Toupin, T. Delahaye, T. Brousse, and D. Belanger, D., "Nanostructured transition metal oxides for aqueous hybrid electrochemical capacitors," *Appl. Phys. A* **82**, 599 (2006).
18. I. E. Rauda, V. Augustyn, B. Dunn, S. H. Tolbert, "Enhancing Pseudocapacitive Charge Storage In Polymer Templated Mesoporous Materials." *Acct. Chem. Res.* **46**, 1113 (2013).
19. K. Brezesinski, J. Wang, J. Haetge, C. Reitz, S. O. Steinmueller, S. H. Tolbert, B. M. Smarsly, B. Dunn, T. Brezesinski, "Pseudocapacitive Contributions to Charge Storage in Highly Ordered Mesoporous Group V Transition Metal Oxides with Iso-Oriented Layered Nanocrystalline Domains." *J. Am. Chem. Soc.* **132**, 6982 (2010).
20. I. E. Rauda, R. Buonsanti, L. C. Saldarriaga-Lopez, K. Benjauthrit, L. T. Schelhas, M. Stefik, V. Augustyn, J. Ko, B. Dunn, U. Wiesner, D. J. Milliron, S. H. Tolbert, "A General Method for the Synthesis of Hierarchical Nanocrystal-Based Mesoporous Materials." *ACS Nano* **6**, 6386 (2012).
21. J. W. Kim, V. Augustyn, and B. Dunn, "The effect of crystallinity on the rapid pseudocapacitive response of Nb_2O_5," *Adv. Energy Mater.* **2,** 141 (2012).
22. V. Augustyn, J. Come, M. A. Lowe, J. W. Kim, P.-L. Taberna, S. H. Tolbert, H. D. Abruña, P. Simon and B. Dunn, "High-rate electrochemical energy storage through Li+ intercalation pseudocapacitance," *Nat. Mater.,* 2013, **12**, 518-522.
23. J. Come, V. Augustyn, J-W. Kim, P. Rozier, P-L. Taberna, P. Gogotsi, J.W. Long, B. Dunn, and P. Simon," Electrochemical kinetics of nanostructured Nb_2O_5 electrodes", submitted for publication.
24. C. Outhwaite, and L. Bhuiyan, "An improved modified Poisson-Boltzmann equation in electric-double-layer theory," *J. Chem. Soc., Faraday Trans*. 2 **79**, 707 (1983).
25. M. Bazant, M. Kilic, B. Storey, and A. Ajdari, "Towards an understanding of induced-charge electrokinetics at large applied voltages in concentrated solutions," *Adv. Colloid Interface Sci.* **152**, 48 (2009).
26. M. Kilic, M. Bazant, and A. Ajdari, "Steric Effects in the Dynamics of Electrolytes at Large Applied Voltages. I. Double-Layer Charging." *Phys. Rev. E* **75**, 021502 (2007).
27. H. Wang and L. Pilon, "Physical Interpretation of Cyclic Voltammetry Measurements," *Electrochim. Acta* **64**, 130-139 (2012).
28. H. Wang and L. Pilon, "Intrinsic Limitations of Impedance Measurements in Determining Electric Double Layer Capacitances," *Electrochim. Acta* **63**, 55–63 (2012).

29. H. Wang and L. Pilon, "Reply to Commentary On Intrinsic Limitations of Impedance Measurements in Determining Electric Double Layer Capacitances," *Electrochim. Acta* **76**, 529-531 (2012).
30. A. L. d'Entremont and L. Pilon, "First Principles Thermal Modeling of Electric Double Layer Capacitors Under Constant-Current Cycling," *J. Power Sources* **246**, 887-898 (2014).
31. A. L. Ayzner, C. J. Tassone, S. H. Tolbert, and B. J. Schwartz, "Reappraising the Need for Bulk Heterojunctions in Polymer/Fullerene Photovoltaics: The Role of Carrier Transport in All-Solution-Processed P3HT/PCBM Bilayer Solar Cells" *J. Phys. Chem. C* **113**, 20050 (2009).
32. A. M. Nardes, A. L. Ayzner, S.R. Hammond, A. J. Ferguson, B. J. Schwartz, and N. Kopidakis, "Photoinduced Charge Carrier Generation and Decay in Sequentially Deposited Polymer/Fullerene Layers: Bulk Heterojunction Vs Planar Interface" *J. Phys. Chem. C* **116**, 7293 (2012).
33. G. Zhang, A. Ferreira, R. Huber, S. D. Boyd, C. K. Luscombe, S. H. Tolbert, and B. J. Schwartz, "Crystallinity Effect in Sequentially-Processed P3HT/PCBM Photovoltaics" *Submitted.*
34. S. A. Hawks, J. C. Aguirre, G. Zhang, R. Thompson, L. T. Schelhas, E. Harris, S. H. Tolbert, and B. J. Schwartz, "On the Composition of Sequentially Solution-Processed Polymer/Fullerene Organic Solar Cell Active Layers" *Submitted.*
35. A. L. Ayzner, S. C. Doan, B. Tremolet de Villers, and B. J. Schwartz, "Ultrafast Studies of Exciton Migration and Polaron Formation in Sequentially Solution-Processed Conjugated Polymer/Fullerene Quasi-Bilayer Photovoltaics" *J. Phys. Chem. Lett.* **3**, 2281 (2012).
36. K. H. Lee, P. E. Schwenn, A. R. G. Smith, H. Cavaye, P. E. Shaw, M. James, K. B. Krueger, I. R. Gentle, P. Meredith, and P. L. Burn, "Morphology of All-Solution-Processed 'Bilayer' Organic Solar Cells" *Adv. Mater.* **23**, 766 (2011).
37. K. H. Lee, Y. Zhang, P. L. Burn, I. R. Gentle, M. James, A. Nelson, and P. Meredith, "Correlation of Diffusion and Performance in Sequentially Processed P3HT/PCBM Heterojunction Films by Time-Resolved Neutron Reflectometry" *J. Mater. Chem. C* **1**, 2593 (2013).
38. H. Chen, S. Hu, H. Zang, B. Hu, and M. Dadmun, "Precise Structural Development and Its Correlation to Function in Conjugated Polymer: Fullerene Thin Films by Controlled Solvent Annealing" *Adv. Funct. Mater.* **23**, 1701 (2013).
39. C. W. Rochester, S. A. Mauger, and A. J. Moule, "Investigating the Morphology of Polymer/Fullerene Layers Coated Using Orthogonal Solvents," *J. Phys. Chem. C* **116**, 7287 (2012).
40. H. M. Daniel, A. Krishnamoorthy, L. N. S. A. Thummalakunta, Y. C. Haw, and L. Joachim, "Formation and Characterisation of Solution Processed 'Pseudo-Bilayer' Organic Solar Cells," *Green* **1** , 291 (2011).
41. V. S. Gevaerts, L. J. A. Koster, M. M. Wienk, R. A. J. Janssen, "Discriminating Between Bilayer and Bulk Heterojunction Polymer:Fullerene Solar Cells Using the External Quantum Efficiency" *ACS Appl. Mater. Interfaces* **3**, 3252 (2011).
42. A. Loiudice, A. Rizzo, G. Latini, C. Nobile, M. de Giorgi, and G. Gigli, "Graded Vertical Phase Separation of Donor/acceptor Species for Polymer Solar Cells" *Sol. Energy Mater. Sol. Cells* **100**, 147 (2012).
43. J. S. Moon, C. J. Takacs, Y. Sun, Y. and A. J. Heeger, "Spontaneous Formation of Bulk Heterojunction Nanostructures: Multiple Routes to Equivalent Morphologies," *Nano Lett.* **11**, 1036 (2011).
44. N. D. Treat, M. A. Brady, G. Smith, M. F. Toney, E. J. Kramer, C. J. Hawker, and M. L. Chabinyc, "Interdiffusion of PCBM and P3HT Reveals Miscibility in a Photovoltaically Active Blend" *Adv. Energy Mater.* **1**, 82 (2011).
45. V. Vohra, G. Arrighetti, L. Barba, K. Higashimine, W. Porzio, and H. Murata, "Enhanced Vertical Concentration Gradient in Rubbed P3HT:PCBM Graded Bilayer Solar Cells," *J. Phys. Chem. Lett.* **3**, 1820 (2012).
46. V. Vohra, K. Higashimine, T. Murakami, and H. Murata, "Addition of Regiorandom Poly (3-Hexylthiophene) to Solution Processed Graded Bilayers to Tune the Vertical Concentration Gradient," *Appl. Phys. Lett.* **101**, 173301 (2012).
47. M. K. Wong and K. Y. Wong, "Investigation of the Factors Affecting the Power Conversion Efficiency of All-Solution-Processed 'bilayer' P3HT:PCBM Solar Cells," *Synth. Met.* 170, **1** (2013).
48. H. Li, Z. Qi, and J. Wang, "Layer-by-Layer Processed Polymer Solar Cells with Self-Assembled Electron Buffer Layer," *Appl. Phys. Lett.* **102**, 213901 (2013).
49. Y. Lin, L. Ma, Y. Li, Y. Liu, D. Zhu, and X. Zhan, "Small-Molecule Solar Cells with Fill Factors up to 0.75 via a Layer-by-Layer Solution Process," *Adv. Energy Mater.* **4**, 1 (2014).
50. D. H. Wang, J. S. Moon, J. Seifter, J. Jo, J. H. Park, O. O. Park, and A. J. Heeger, "Sequential Processing: Control of Nanomorphology in Bulk Heterojunction Solar Cells," *Nano Lett.* **11**, 3163 (2011).

51. H. Y. Yang, N. S. Kang, J.-M. Hong, Y.-W. Song, T. W., Kim, and J. A. Lim, "Efficient Bilayer Heterojunction Polymer Solar Cells with Bumpy Donor-Acceptor Interface Formed by Facile Polymer Blend," *Org. Electron.* **13**, 2688 (2012).
52. R. Zhu, A. Kumar, and Y. Yang, "Polarizing Organic Photovoltaics," *Adv. Mater.* **23**, 4193 (2011).
53. H. Li, Z. Zhang, Y. Li, and J. Wang, "Tunable Open-Circuit Voltage in Ternary Organic Solar Cells," *Appl. Phys. Lett.* **101**, 163302 (2012).
54. D. Wang, J. Kim, O. Park, and J. Park, "Analysis of Surface Morphological Changes in Organic Photovoltaic Devices: Bilayer Versus Bulk-Heterojunction," *Energy Environ. Sci.* **4**, 1434 (2011).
55. B. Liu, R.-Q. Png, L.-H. Zhao, L.-L. Chua, R. H. Friend, and P. K. H. Ho, "High Internal Quantum Efficiency in Fullerene Solar Cells Based on Crosslinked Polymer Donor Networks," *Nat. Commun.* **3**, 1321 (2012).
56. A. Loiudice, A. Rizzo, M. Biasiucci, and G. Gigli, "Bulk Heterojunction Versus Diffused Bilayer: The Role of Device Geometry in Solution p-Doped Polymer-Based Solar Cells," *J. Phys. Chem. Lett.* **3**, 1908 (2012).
57. H. Park, J. Lee, T. Lee, and L. Guo, "Advanced Heterojunction Structure of Polymer Photovoltaic Cell Generating High Photocurrent with Internal Quantum Efficiency Approaching 100%," *Adv. Energy Mater.* 3, 1135 (2013).
58. L. N. S. A. Thummalakunta, C. H. Yong, K. Ananthanarayanan, and J. Luther, "P3HT Based Solution-Processed Pseudo Bi-Layer Organic Solar Cell with Enhanced Performance," *Org. Electron.* **13**, 2008 (2012).
59. D. H. Wang, H. K. Lee, D.-G. Choi, J. H. Park, and O. O. Park, "Solution-Processable Polymer Solar Cells from a Poly(3-Hexylthiophene)/[6,6]-Phenyl C61-Butyric Acidmethyl Ester Concentration Graded Bilayers," *Appl. Phys. Lett.* **95**, 043505 (2009).
60. A. L. Ayzner, C. J. Tassone, S. H. Tolbert, and B. J. Schwartz, "Reappraising the Need for Bulk Heterojunctions in Polymer/Fullerene Photovoltaics: The Role of Carrier Transport in All-Solution-Processed P3HT/PCBM Bilayer Solar Cells," *J. Phys. Chem. C* **113**, 20050 (2009).
61. G. Zhang, A. Ferreira, R. Huber, S. D. Boyd, C. K. Luscombe, S. H. Tolbert, and B. J. Schwartz, "Crystallinity Effect in Sequentially-Processed P3HT/PCBM Photovoltaics" *Submitted.*
62. N. C. Miller, E. Cho, M. J. N. Junk, R. Gysel, C. Risko, D. Kim, S. Sweetnam, C. E. Miller, L. J. Richter, R. J. Kline, M. Heeney, I. McCulloch, A. Amassian, D. Acevedo-Feliz, C. Knox, M. R. Hansen, D. Dudenko, B. F. Chmelka, M. F. Toney, J.-L. Brédas, and M. D. McGehee, "Use of X-Ray Diffraction, Molecular Simulations, and Spectroscopy to Determine the Molecular Packing in a Polymer-Fullerene Bimolecular Crystal," *Adv. Mater.* **24**, 6071 (2012).
63. D. Chen, F. Liu, C. Wang, A. Nakahara, and T. P. Russell, "Bulk Heterojunction Photovoltaic Active Layers via Bilayer," *Nano Lett.* **11**, 2071 (2011).
64. B. Collins, E. Gann, L. Guignard, X. He, C. R. McNeill, and H. Ade, "Molecular Miscibility of Polymer Fullerene Blends," *J. Phys. Chem. Lett.* 1, 3160 (2010).
65. H. A. Bronstein. and C. K. Luscombe, "Externally Initiated Regioregular P3HT with Controlled Molecular Weight and Narrow Polydispersity," *J. Am. Chem. Soc.* **131**, 12894 (2009).
66. R. D. Kennedy, A. L. Ayzner, D. D. Wanger, C. T. Day, M. Halim, S. I. Khan, S. H. Tolbert, B. J. Schwartz, and Y. Rubin, "Self-Assembling Fullerenes for Improved Bulk-Heterojunction Photovoltaic Devices," *J. Am. Chem. Soc.* **130**, 17290 (2008).
67. M. Sawamura, K. Kawai, Y. Matsuo, K. Kanie, T. Kato, and E. Nakamura, "Stacking of Conical Molecules with a Fullerene Apex into Polar Columns in Crystals and Liquid Crystals" *Nature* **419**, 702 (2002).
68. Y. Matsuo, Y. Sato, M. Hashiguchi, K. Matsuo, and E. Nakamura, "Synthesis, Electrochemical and Photophysical Properties, and Electroluminescent Performance of the Octa- and Deca(aryl)[60]fullerene Derivatives," *Adv. Funct. Mater.* **19**, 2224 (2009).
69. Y. Matsuo, A. Muramatsu, R. Hamasaki, N. Mizoshita, T. Kato, and E. Nakamura, "Stacking of Molecules Possessing a Fullerene Apex and a Cup-Shaped Cavity Connected by a Silicon Connection," *J. Am. Chem. Soc.* **126**, 432 (2003).
70. R. D. Kennedy, M. Halim, S. I. Khan, B. J. Schwartz, S. H. Tolbert, and Y. Rubin, "Crystal-Packing Trends for a Series of 6,9,12,15,18-Pentaaryl-1-Hydro[60]fullerenes," *Chem. Eur. J.* **18**, 7418 (2012).
71. C. J. Tassone, A. L. Ayzner, R. D. Kennedy, M. Halim, M. So, Y. Rubin, S. H. Tolbert, and B. J. Schwartz, "Using Pentaarylfullerenes to Understand Network Formation in Conjugated Polymer-Based Bulk-Heterojunction Solar Cells," *J. Phys. Chem. C* **115**, 22563 (2011).
72. J. C. Aguirre, C. Arntsen, S. Hernandez, R. Huber, A. M. Nardes, M. Halim, D. Kilbride, N. Kopidakis, S. H. Tolbert, B. J. Schwartz, and N. Daniel, "Understanding Local and Macroscopic Electron Mobilities in the Fullerene Network of Conjugated Polymer-Based Solar Cells: Time-Resolved Microwave Conductivity and Theory," *Adv. Funct. Mater.* DOI: 10.1002/adfm.201301757 (2013).

73. A. P. Clark, C. Shi, B. C. Ng, J. N. Wilking, A. L. Ayzner, A. Z. Stieg, B. J. Schwartz, T. G. Mason, Y. Rubin, S. H. Tolbert, and C. E. Al, "Self-Assembling Semiconducting Polymers: Rods and Gels from Electronic Materials," *ACS Nano* **7**, 962 (2013).
74. A. J. Cadby and S. H. Tolbert, "Controlling Optical Properties and Interchain Interactions in Semiconducting Polymers by Encapsulation in Periodic Nanoporous Silicas with Different Pore Sizes," *J. Phys. Chem. B* **109**, 17879 (2005).

2 LIST OF PEER-REVIEWED PUBLICATIONS

We have published 94 journal-refereed papers, which give full details of our technical accomplishments. Below is a full list as of the date of this report.

1. Adelstein, N., Neaton, J. B., Asta, M., & De Jonghe, L. C. (2014). Density functional theory based calculation of small-polaron mobility in hematite. *Physical Review B, 89*(24), 245115. doi:10.1103/PhysRevB.89.245115

2. Aguirre, J. C., Arntsen, C., Hernandez, S., Huber, R., Nardes, A. M., Halim, M., . . . Neuhauser, D. (2014). Understanding local and macroscopic electron mobilities in the fullerene network of conjugated polymer-based solar cells: Time-resolved microwave conductivity and theory. *Advanced Functional Materials, 24*(6), 784-792. doi:10.1002/adfm.201301757

3. Aguirre, J. C., Ferreira, A., Ding, H., Jenekhe, S. A., Kopidakis, N., Asta, M., . . . Ozolins, V. (2014). Panoramic view of electrochemical pseudocapacitor and organic solar cell research in molecularly engineered energy materials (MEEM). *Journal of Physical Chemistry C, 118*(34), 19505-19523. doi:10.1021/jp501047j

4. Aguirre, J. C., Hawks, S. A., Ferreira, A. S., Yee, P., Subramaniyan, S., Jenekhe, S. A., . . . Schwartz, B. J. (2015). Sequential processing for organic photovoltaics: Design rules for morphology control by tailored semi-orthogonal solvent blends.*Advanced Energy Materials, 5*(11), 1402020. doi:10.1002/aenm.201402020

5. Armin, A., Jansen-van Vuuren, R. D., Kopidakis, N., Burn, P. L., & Meredith, P. (2015). Narrowband light detection via internal quantum efficiency manipulation of organic photodiodes. *Nature Communications, 6*, 6343. doi:10.1038/ncomms7343

6. Arntsen, C., Reslan, R., Hernandez, S., Gao, Y., & Neuhauser, D. (2013). Direct delocalization for calculating electron transfer in fullerenes. *International Journal of Quantum Chemistry, 113*(15), 1885-1889. doi:10.1002/qua.24409

7. Ayzner, A. L., Doan, S. C., de Villers, B. T., & Schwartz, B. J. (2012). Ultrafast studies of exciton migration and polaron formation in sequentially solution-processed conjugated Polymer/Fullerene quasi-bilayer photovoltaics. *Journal of Physical Chemistry Letters, 3*(16), 2281-2287. doi:10.1021/jz300762c

8. Ayzner, A. L., Mei, J., Appleton, A., DeLongchamp, D., Nardes, A., Benight, S., . . . Bao, Z. (2015). Impact of the crystallite orientation distribution on exciton transport in donor-acceptor conjugated polymers. *Acs Applied Materials & Interfaces,7*(51), 28035-28041. doi:10.1021/acsami.5b02968

9. Baer, R., Neuhauser, D., & Rabani, E. (2013). Self-averaging stochastic kohn-sham density-functional theory. *Physical Review Letters, 111*(10), 106402. doi:10.1103/PhysRevLett.111.106402

10. Bartell, L. A., Wall, M. R., & Neuhauser, D. (2010). A time-dependent semiempirical approach to determining excited states. *Journal of Chemical Physics, 132*(23), 234106. doi:10.1063/1.3453683

11. Brezesinski, K., Haetge, J., Wang, J., Mascotto, S., Reitz, C., Rein, A., . . . Brezesinski, T. (2011). Ordered mesoporous alpha-Fe2O3 (hematite) thin-film electrodes for application in high rate rechargeable lithium batteries. *Small, 7*(3), 407-414. doi:10.1002/smll.201001333

12. Brezesinski, K., Wang, J., Haetge, J., Reitz, C., Steinmueller, S. O., Tolbert, S. H., . . . Brezesinski, T. (2010). Pseudocapacitive contributions to charge storage in highly ordered mesoporous group V transition metal oxides with iso-oriented layered nanocrystalline domains. *Journal of the American Chemical Society, 132*(20), 6982-6990. doi:10.1021/ja9106385

13. Brezesinski, T., Wang, J., Senter, R., Brezesinski, K., Dunn, B., & Tolbert, S. H. (2010). On the correlation between mechanical flexibility, nanoscale structure, and charge storage in periodic mesoporous CeO2 thin films. *Acs Nano, 4*(2), 967-977. doi:10.1021/nn9007324

14. Chen, Z., Augustyn, V., Wen, J., Zhang, Y., Shen, M., Dunn, B., & Lu, Y. (2011). High-performance supercapacitors based on intertwined CNT/V2O5 nanowire nanocomposites. *Advanced Materials, 23*(6), 791-+. doi:10.1002/adma.201003658

15. Chen, Z., Wen, J., Yan, C., Rice, L., Sohn, H., Shen, M., . . . Lu, Y. (2011). High-performance supercapacitors based on hierarchically porous graphite particles. *Advanced Energy Materials, 1*(4), 551-556. doi:10.1002/aenm.201100114

16. Chen, Z., Weng, D., Wang, X., Cheng, Y., Wang, G., & Lu, Y. (2012). Ready fabrication of thin-film electrodes from building nanocrystals for micro-supercapacitors. *Chemical Communications, 48*(31), 3736-3738. doi:10.1039/c2cc30406f

17. Chuang, F., Hsu, C., Chen, C., Huang, Z., Ozolins, V., Lin, H., & Bansil, A. (2013). Tunable topological electronic structures in sb(111) bilayers: A first-principles study. *Applied Physics Letters, 102*(2), 022424. doi:10.1063/1.4776734

18. Chuang, F., Lin, W., Huang, Z., Hsu, C., Kuo, C., Ozolins, V., & Yeh, V. (2011). Electronic structures of an epitaxial graphene monolayer on SiC(0001) after gold intercalation: A first-principles study. *Nanotechnology, 22*(27), 275704. doi:10.1088/0957-4484/22/27/275704

19. Clark, A. P., Shi, C., Ng, B. C., Wilking, J. N., Ayzner, A. L., Stieg, A. Z., . . . Tolbert, S. H. (2013). Self-assembling semiconducting polymers-rods and gels from electronic materials. *Acs Nano, 7*(2), 962-977. doi:10.1021/nn304437k

20. Cook, J. B., Kim, H., Yan, Y., Ko, J. S., Robbennolt, S., Dunn, B., & Tolbert, S. H. (2016). Mesoporous MoS2 as a transition metal dichalcogenide exhibiting pseudocapacitive li and na-ion charge storage. *Advanced Energy Materials, 6*(9), 1501937. doi:10.1002/aenm.201501937

21. d'Entremont, A. L., Girard, H., Wang, H., & Pilon, L. (2016). Electrochemical transport phenomena in hybrid pseudocapacitors under galvanostatic cycling. *Journal of the Electrochemical Society, 163*(2), A229-A243. doi:10.1149/2.0441602jes

22. d'Entremont, A. L., & Pilon, L. (2015). Thermal effects of asymmetric electrolytes in electric double layer capacitors. *Journal of Power Sources, 273*, 196-209. doi:10.1016/j.jpowsour.2014.09.080

23. d'Entremont, A., & Pilon, L. (2014). Scaling laws for heat generation and temperature oscillations in EDLCs under galvanostatic cycling. *International Journal of Heat and Mass Transfer, 75*, 637-649. doi:10.1016/j.ijheatmasstransfer.2014.04.001

24. d'Entremont, A., & Pilon, L. (2014). First-order thermal model of commercial EDLCs. *Applied Thermal Engineering, 67*(1-2), 439-446. doi:10.1016/j.applthermaleng.2014.03.061

25. d'Entremont, A., & Pilon, L. (2014). First-principles thermal modeling of electric double layer capacitors under constant-current cycling. *Journal of Power Sources, 246*, 887-898. doi:10.1016/j.jpowsour.2013.08.024

26. Detsi, E., Cook, J. B., Lesel, B. K., Turner, C. L., Liang, Y., Robbennolt, S., & Tolbert, S. H. (2016). Mesoporous Ni60Fe30Mn10-alloy based metal/metal oxide composite thick films as highly active and robust oxygen evolution catalysts. *Energy & Environmental Science, 9*(2), 540-549. doi:10.1039/c5ee02509e

27. Ding, H., Lin, H., Sadigh, B., Zhou, F., Ozolins, V., & Asta, M. (2014). Computational investigation of electron small polarons in alpha-MoO3. *Journal of Physical Chemistry C, 118*(29), 15565-15572. doi:10.1021/jp503065x

28. Ding, H., Ray, K. G., Ozolins, V., & Asta, M. (2012). Structural and vibrational properties of alpha-MoO3 from van der waals corrected density functional theory calculations. *Physical Review B, 85*(1), 012104. doi:10.1103/PhysRevB.85.012104

29. Ding, H., & Xu, B. (2012). Structural, elastic, and vibrational properties of layered titanium dichalcogenides: A van der waals density functional study. *Journal of Chemical Physics, 137*(22), 224509. doi:10.1063/1.4770293

30. Earmme, T., Hwang, Y., Subramaniyan, S., & Jenekhe, S. A. (2014). All-polymer bulk heterojuction solar cells with 4.8% efficiency achieved by solution processing from a co-solvent. *Advanced Materials, 26*(35), 6080-+. doi:10.1002/adma.201401490

31. Fang, J., Kang, C. B., Huang, Y., Tolbert, S. H., & Pilon, L. (2012). Thermal conductivity of ordered mesoporous nanocrystalline silicon thin films made from magnesium reduction of polymer-templated silica. *Journal of Physical Chemistry C,116*(23), 12926-12933. doi:10.1021/jp302531d

32. Fang, Y., Pandey, A. K., Nardes, A. M., Kopidakis, N., Burn, P. L., & Meredith, P. (2013). A narrow optical gap small molecule acceptor for organic solar cells. *Advanced Energy Materials, 3*(1), 54-59. doi:10.1002/aenm.201200372

33. Fei, L., Xu, Y., Chen, Z., Yuan, B., Wu, X., Hill, J., . . . Luo, H. (2013). Preparation of porous SnO2 helical nanotubes and SnO2 sheets. *Materials Chemistry and Physics, 140*(1), 249-254. doi:10.1016/j.matchemphys.2013.03.029

34. Finck, B. Y., & Schwartz, B. J. (2015). Drift-diffusion modeling of the effects of structural disorder and carrier mobility on the performance of organic photovoltaic devices. *Physical Review Applied, 4*(3), 034006. doi:10.1103/PhysRevApplied.4.034006

35. Gao, Y., Neuhauser, D., Baer, R., & Rabani, E. (2015). Sublinear scaling for time-dependent stochastic density functional theory. *Journal of Chemical Physics, 142*(3), 034106. doi:10.1063/1.4905568

36. Girard, H., Wang, H., d'Entremont, A. L., & Pilon, L. (2015). Enhancing faradaic charge storage contribution in hybrid pseudocapacitors. *Electrochimica Acta, 182*, 639-651. doi:10.1016/j.electacta.2015.09.070

37. Girard, H., Wang, H., d'Entremont, A., & Pilon, L. (2015). Physical interpretation of cyclic voltammetry for hybrid pseudocapacitors. *Journal of Physical Chemistry C, 119*(21), 11349-11361. doi:10.1021/acs.jpcc.5b00641

38. Halim, M., Kennedy, R. D., Suzuki, M., Khan, S. I., Diaconescu, P. L., & Rubin, Y. (2011). Complexes of gold(I), silver(I), and copper(I) with pentaaryl[60]fullerides. *Journal of the American Chemical Society, 133*(17), 6841-6851. doi:10.1021/ja201297r

39. Hawks, S. A., Aguirre, J. C., Schelhas, L. T., Thompson, R. J., Huber, R. C., Ferreira, A. S., . . . Schwartz, B. J. (2014). Comparing matched polymer:Fullerene solar cells made by solution-sequential processing and traditional blend casting: Nanoscale structure and device performance. *Journal of Physical Chemistry C, 118*(31), 17413-17425. doi:10.1021/jp504560r

40. Hawks, S. A., Finck, B. Y., & Schwartz, B. J. (2015). Theory of current transients in planar semiconductor devices: Insights and applications to organic solar cells. *Physical Review Applied, 3*(4), 044014. doi:10.1103/PhysRevApplied.3.044014

41. Hawks, S. A., Li, G., Yang, Y., & Street, R. A. (2014). Band tail recombination in polymer: Fullerene organic solar cells. *Journal of Applied Physics, 116*(7), 074503. doi:10.1063/1.4892869

42. Hmadeh, M., Lu, Z., Liu, Z., Gandara, F., Furukawa, H., Wan, S., . . . Yaghi, O. M. (2012). New porous crystals of extended metal-catecholates. *Chemistry of Materials, 24*(18), 3511-3513. doi:10.1021/cm301194a

43. Houndonougbo, Y., Signer, C., He, N., Morris, W., Furukawa, H., Ray, K. G., . . . Yaghi, O. M. (2013). A combined experimental-computational investigation of methane adsorption and selectivity in a series of isoreticular zeolitic imidazolate frameworks. *Journal of Physical Chemistry C, 117*(20), 10326-10335. doi:10.1021/jp3096192

44. Hsu, C., Chang, H., Chuang, F., Liu, Y., Huang, Z., Lin, H., . . . Bansil, A. (2014). First-principles study of atomic structures and electronic properties of ultrathin bi films on ge(111). *Surface Science, 626*, 68-75. doi:10.1016/j.susc.2014.03.024

45. Hsu, C., Lin, W., Ozolins, V., & Chuang, F. (2012). Electronic structure of the indium-adsorbed Au/Si(111)-root 3 x root 3 surface: A first-principles study. *Physical Review B, 85*(15), 155401. doi:10.1103/PhysRevB.85.155401

46. Hsu, C., Lin, W., Ozolins, V., & Chuang, F. (2012). Electronic structures of an epitaxial graphene monolayer on SiC(0001) after metal intercalation (metal = al, ag, au, pt, and pd): A first-principles study. *Applied Physics Letters, 100*(6), 063115. doi:10.1063/1.3682303

47. Hsu, C., Ozolins, V., & Chuang, F. (2013). First-principles study of bi and sb intercalated graphene on SiC(0001) substrate. *Surface Science, 616*, 149-154. doi:10.1016/j.susc.2013.06.002

48. Huber, R. C., Ferreira, A. S., Aguirre, J. C., Kilbride, D., Toso, D. B., Mayoral, K., . . . Tolbert, S. H. (2016). Structure and conductivity of semiconducting polymer hydrogels. *Journal of Physical Chemistry B, 120*(26), 6215-6224. doi:10.1021/acs.jpcb.6b02202

49. Hwang, Y., Courtright, B. A. E., Ferreira, A. S., Tolbert, S. H., & Jenekhe, S. A. (2015). 7.7% efficient all-polymer solar cells. *Advanced Materials, 27*(31), 4578-4584. doi:10.1002/adma.201501604

50. Jia, X., Chen, Z., Suwarnasarn, A., Rice, L., Wang, X., Sohn, H., . . . Lu, Y. (2012). High-performance flexible lithium-ion electrodes based on robust network architecture. *Energy & Environmental Science, 5*(5), 6845-6849. doi:10.1039/c2ee03110h

51. Jia, X., Yan, C., Chen, Z., Wang, R., Zhang, Q., Guo, L., . . . Lu, Y. (2011). Direct growth of flexible LiMn2O4/CNT lithium-ion cathodes. *Chemical Communications, 47*(34), 9669-9671. doi:10.1039/c1cc13536h

52. Kennedy, R. D., Halim, M., Khan, S. I., Schwartz, B. J., Tolbert, S. H., & Rubin, Y. (2012). Crystal-packing trends for a series of 6,9,12,15,18-pentaaryl-1-hydro[60]fullerenes. *Chemistry-a European Journal, 18*(24), 7418-7433. doi:10.1002/chem.201103400

53. Ko, S., Kim, D. H., Ayzner, A. L., Mannsfeld, S. C. B., Verploegen, E., Nardes, A. M., . . . Bao, Z. (2015). Thermotropic phase transition of benzodithiophene copolymer thin films and its impact on electrical and photovoltaic characteristics.*Chemistry of Materials, 27*(4), 1223-1232. doi:10.1021/cm503773j

54. Kurihara, H., Iiduka, Y., Rubin, Y., Waelchli, M., Mizorogi, N., Slanina, Z., . . . Akasaka, T. (2012). Unexpected formation of a Sc3C2@C-80 bisfulleroid derivative. *Journal of the American Chemical Society, 134*(9), 4092-4095. doi:10.1021/ja300279x

55. Li, G., Wang, X., Chen, Z., Ma, X., & Lu, Y. (2013). Characterization of niobium and vanadium oxide nanocomposites with improved rate performance and cycling stability. *Electrochimica Acta, 102*, 351-357. doi:10.1016/j.electacta.2013.03.169

56. Lin, H., Zhou, F., Liu, C., & Ozolins, V. (2014). Non-grotthuss proton diffusion mechanism in tungsten oxide dihydrate from first-principles calculations. *Journal of Materials Chemistry a, 2*(31), 12280-12288. doi:10.1039/c4ta02465f

57. Liu, Y., & Ozolins, V. (2012). Self-assembled monolayers on au(111): Structure, energetics, and mechanism of reconstruction lifting. *Journal of Physical Chemistry C, 116*(7), 4738-4747. doi:10.1021/jp211407p

58. Liu, Y., & Ozolins, V. (2011). Diffusion-assisted formation mechanism of molecular break junctions: A first-principles study of benzenethiolate on au(111). *Journal of Physical Chemistry C, 115*(8), 3460-3465. doi:10.1021/jp110072w

59. Liu, Y., Zhou, F., & Ozolins, V. (2012). Ab initio study of the charge-storage mechanisms in RuO2-based electrochemical ultracapacitors. *Journal of Physical Chemistry C, 116*(1), 1450-1457. doi:10.1021/jp207616s

60. Morris, W., He, N., Ray, K. G., Klonowski, P., Furukawa, H., Daniels, I. N., . . . Laird, B. B. (2012). A combined experimental-computational study on the effect of topology on carbon dioxide adsorption in zeolitic imidazolate frameworks. *Journal of Physical Chemistry C, 116*(45), 24084-24090. doi:10.1021/jp307170a

61. Morris, W., Leung, B., Furukawa, H., Yaghi, O. K., He, N., Hayashi, H., . . . Yaghi, O. M. (2010). A combined experimental-computational investigation of carbon dioxide capture in a series of isoreticular zeolitic imidazolate frameworks. *Journal of the American Chemical Society, 132*(32), 11006-11008. doi:10.1021/ja104035j

62. Morris, W., Stevens, C. J., Taylor, R. E., Dybowski, C., Yaghi, O. M., & Garcia-Garibay, M. A. (2012). NMR and X-ray study revealing the rigidity of zeolitic imidazolate frameworks. *Journal of Physical Chemistry C, 116*(24), 13307-13312. doi:10.1021/jp303907p

63. Muller, G. A., Cook, J. B., Kim, H., Tolbert, S. H., & Dunn, B. (2015). High performance pseudocapacitor based on 2D layered metal chalcogenide nanocrystals. *Nano Letters, 15*(3), 1911-1917. doi:10.1021/nl504764m

64. Nardes, A. M., Ayzner, A. L., Hammond, S. R., Ferguson, A. J., Schwartz, B. J., & Kopidakis, N. (2012). Photoinduced charge carrier generation and decay in sequentially deposited Polymer/Fullerene layers: Bulk heterojunction vs planar interface. *Journal of Physical Chemistry C, 116*(13), 7293-7305. doi:10.1021/jp212390p

65. Nardes, A. M., Ferguson, A. J., Whitaker, J. B., Larson, B. W., Larsen, R. E., Maturova, K., . . . Kopidakis, N. (2012). Beyond PCBM: Understanding the photovoltaic performance of blends of indene-C60 multiadducts with poly(3-hexylthiophene).*Advanced Functional Materials, 22*(19), 4115-4127. doi:10.1002/adfm.201200336

66. Nardes, A. M., Ferguson, A. J., Wolfer, P., Gui, K., Burn, P. L., Meredith, P., & Kopidakis, N. (2014). Free carrier generation in organic photovoltaic bulk heterojunctions of conjugated polymers with molecular acceptors: Planar versus spherical acceptors. *Chemphyschem, 15*(8), 1539-1549. doi:10.1002/cphc.201301022

67. Neuhauser, D., Gao, Y., Arntsen, C., Karshenas, C., Rabani, E., & Baer, R. (2014). Breaking the theoretical scaling limit for predicting quasiparticle energies: The stochastic GW approach. *Physical Review Letters, 113*(7), 076402. doi:10.1103/PhysRevLett.113.076402

68. Neuhauser, D., Rabani, E., & Baer, R. (2013). Expeditious stochastic calculation of random-phase approximation energies for thousands of electrons in three dimensions. *Journal of Physical Chemistry Letters, 4*(7), 1172-1176. doi:10.1021/jz3021606

69. Ozolins, V., Zhou, F., & Asta, M. (2013). Ruthenia-based electrochemical supercapacitors: Insights from first-principles calculations. *Accounts of Chemical Research, 46*(5), 1084-1093. doi:10.1021/ar3002987

70. Peng, Y., Chen, Z., Wen, J., Xiao, Q., Weng, D., He, S., . . . Lu, Y. (2011). Hierarchical manganese Oxide/Carbon nanocomposites for supercapacitor electrodes. *Nano Research, 4*(2), 216-225. doi:10.1007/s12274-010-0072-y

71. Pilon, L., Wang, H., & d'Entremont, A. (2015). Recent advances in continuum modeling of interfacial and transport phenomena in electric double layer capacitors. *Journal of the Electrochemical Society, 162*(5), A5158-A5178. doi:10.1149/2.0211505jes

72. Rauda, I. E., Augustyn, V., Saldarriaga-Lopez, L. C., Chen, X., Schelhas, L. T., Rubloff, G. W., . . . Tolbert, S. H. (2014). Nanostructured pseudocapacitors based on atomic layer deposition of V2O5 onto conductive nanocrystal-based mesoporous ITO scaffolds. *Advanced Functional Materials, 24*(42), 6717-6728. doi:10.1002/adfm.201401284

73. Rauda, I. E., Buonsanti, R., Saldarriaga-Lopez, L. C., Benjauthrit, K., Schelhas, L. T., Stefik, M., . . . Tolbert, S. H. (2012). General method for the synthesis of hierarchical nanocrystal-based mesoporous materials. *Acs Nano, 6*(7), 6386-6399. doi:10.1021/nn302789r

74. Rauda, I. E., Saldarriaga-Lopez, L. C., Helms, B. A., Schelhas, L. T., Membreno, D., Milliron, D. J., & Tolbert, S. H. (2013). Nanoporous semiconductors synthesized through polymer templating of ligand-stripped CdSe nanocrystals. *Advanced Materials, 25*(9), 1315-1322. doi:10.1002/adma.201203309

75. Rauda, I. E., Senter, R., & Tolbert, S. H. (2013). Directing anisotropic charge transport of layered organic-inorganic hybrid perovskite semiconductors in porous templates. *Journal of Materials Chemistry C, 1*(7), 1423-1427. doi:10.1039/c2tc00239f

76. Ray, K. G., Olmsted, D. L., Burton, J. M. R., Houndonougbo, Y., Laird, B. B., & Asta, M. (2014). Gas membrane selectivity enabled by zeolitic lmidazolate framework electrostatics. *Chemistry of Materials, 26*(13), 3976-3985. doi:10.1021/cm5015477

77. Ray, K. G., Olmsted, D. L., Houndonougbo, Y., Laird, B. B., & Asta, M. (2013). Origins of CH4/CO2 adsorption selectivity in zeolitic imidazolate frameworks: A van der waals density functional study. *Journal of Physical Chemistry C, 117*(28), 14642-14651. doi:10.1021/jp404251m

78. Ray, K. G., Olmsted, D., He, N., Houndonougbo, Y., Laird, B. B., & Asta, M. (2012). Van der waals density functional study of CO2 binding in zeolitic imidazolate frameworks. *Physical Review B, 85*(8), 085410. doi:10.1103/PhysRevB.85.085410

79. Reslan, R., Lopata, K., Arntsen, C., Govind, N., & Neuhauser, D. (2012). Electron transfer beyond the static picture: A TDDFT/TD-ZINDO study of a pentacene dimer. *Journal of Chemical Physics, 137*(22), 22A502. doi:10.1063/1.4729047

80. Savenije, T. J., Ferguson, A. J., Kopidakis, N., & Rumbles, G. (2013). Revealing the dynamics of charge carriers in polymer:Fullerene blends using photoinduced time-resolved microwave conductivity. *Journal of Physical Chemistry C, 117*(46), 24085-24103. doi:10.1021/jp406706u

81. Street, R. A., Hawks, S. A., Khlyabich, P. P., Li, G., Schwartz, B. J., Thompson, B. C., & Yang, Y. (2014). Electronic structure and transition energies in polymer-fullerene bulk heterojunctions. *Journal of Physical Chemistry C, 118*(38), 21873-21883. doi:10.1021/jp507097h